

Selective Castration-resistant Prostate Cancer Photothermal Ablation With Copper Sulfide Nanoplates



Jun Chen¹, Zhao-jie Wang¹, Kai-le Zhang¹, Yan-jun Xu, Zhi-gang Chen, and Xiao-yong Hu

OBJECTIVE	To explore new therapies for castration-resistant prostate cancer to improve patients' quality of life and extend life.
MATERIALS AND METHODS	The synthesis, morphology analysis, phase analysis, spectral analysis, and photothermal conversion test were referenced to our previous articles. Then near-infrared light-driven copper sulfide (CuS) nanoplates to inhibit the growth of prostate cancer cells in vivo and in vitro was carried out. Transmission electron microscope, mCherry-LC3 syncytial virus labeling, acridine orange staining, and autophagy protein were used to detect the autophagy caused by CuS nanoplates and chloroquine was used to inhibit the process of autophagy.
RESULTS	The CuS nanoplates prepared in this study feature low cytotoxicity, simple preparation, and high photothermal conversion efficiency. Driven by 980 nm near-infrared light, CuS nanoplates could inhibit the growth of prostate cancer cells in vivo and in vitro, while triggering the autophagy and cytoprotection of prostate cancer cells.
CONCLUSION	CuS nanoplates are a kind of commendable photothermal therapy agent in castration-resistant prostate cancer treating. Autophagy inhibition enhances the photothermal efficiency of CuS nanoplates, which indicates favorable application prospects in the treatment of advanced prostate cancer. UROLOGY 125: 248–255, 2019. © 2018 Elsevier Inc.

Prostate cancer is a major threat to the health of men in Western countries,¹ and the incidence of prostate cancer in China has been on an upward trajectory year by year.² Although there are a variety of options for prostate cancer treatment, including radical surgery, radiotherapy, and androgen deprivation therapy, recurrent and metastatic prostate cancer will be eventually in progress to "castration-resistant prostate cancer (CRPC)." Bone metastases will occur in 90% of CRPC cases and become the main cause of death of prostate

cancer patients.³ Metastatic castration-resistant prostate cancer (mCRPC) is the most intractable stage in the treatment of prostate cancer. In the past, the priority was given to chemotherapy for mCRPC treatment, that is, Docetaxel, with about 3 months median survival time.⁴ Recently, various new drugs treating prostate cancer have sprung into existence successively, including "Radium-223,"⁵ "Enzalutamide/MDV3100,"⁶ and "Abiraterone,"⁷ with 3.6 months, 4.8 months, and 3.9 months median survival time, respectively. Therefore, it is crucial to further explore new mCRPC therapies to prolong patients' life and improve their quality of life.

The mCRPC therapy emphasizes inhibiting the progression of the primary lesion and bone metastatic lesions of prostate cancer. These 2 types of lesions are closer to the body surface or rectum cavity, providing convenience for photothermal therapy. Photothermal therapy converts laser light energy into heat energy by utilizing photothermal conversion materials to kill cancer cells under the achieved local high temperature. It features minimal invasion, low treatment cost, and targeting, which is the most promising treatment program for solid tumor following surgery, radiotherapy, chemotherapy, and biological therapy.⁸ In theory, phototherapy enjoys a desirable prospect in the treatment of mCRPC.

¹ Contributed equally to this work.

Funding Support: This work was funded by State Key Laboratory for Modification of Chemical Fibers and Polymer Materials of Donghua University, China (LK1524); National Natural Science Foundation of China (Grant Nos. 51473033, 51773036, 81700590); Science and Technology Commission of Shanghai Municipality for the support under the International Collaboration Project (17410742800); Natural Science Foundation of Shanghai (18ZR1401700).

Abstract

From the Department of Urology, Affiliated Sixth People's Hospital, Shanghai Jiao Tong University, Shanghai, China; the State Key Laboratory for Modification of Chemical Fibers and Polymer Materials, College of Materials Science and Engineering, Donghua University, Shanghai, China; the Department of Ultrasound in Medicine, Affiliated Sixth People's Hospital, Shanghai Jiao Tong University, Shanghai, China; and the Shanghai Eastern Institute for Urologic Repair and Reconstruction, Shanghai, China

Address correspondence to: Xiao-yong Hu, MD, PhD, Department of Urology, Affiliated Sixth People's Hospital, Shanghai Jiao Tong University, Yishan Road 600, Xuhui District, Shanghai 200233, China. E-mail: xiaoyonghu@126.com

Submitted: July 21, 2018, accepted (with revisions): November 13, 2018

The top priority for photothermal therapy is to select the appropriate light source. Compared with visible light (wavelength of 350-650 nm) and infrared light (wavelength greater than 1000 nm), near-infrared (NIR) light (wavelength of 650-1000 nm) dominates by less energy attenuation and strong tissue penetration effect when passing through biological tissues,⁹ serving as the optimal choice for photothermal therapy. Another important task of photothermal therapy is to screen the appropriate photothermal conversion material. At present, the photothermal conversion materials of ongoing research mainly include: noble metal-based photothermal conversion materials, carbon-based photothermal conversion materials, organic compound photothermal conversion materials, and copper sulfide (CuS)-based photothermal conversion materials. We have made productive investigations in the field of CuS-based photothermal conversion material, and when compared with the former materials, CuS-based photothermal conversion materials are superior for their simple preparation, high-absorption coefficient, low-cost, and easy to be modified.^{10,11} It was found that NIR-light-driven CuS nanoplates could significantly inhibit the growth of prostate cancer cells. Nanoplates often cause autophagy of cells in tumor treatment, which is commonly seen in the body's physiological and pathologic processes. The mechanism and role of autophagy caused by nanoplates have not yet fully elucidated. Autophagy cannot only enhance the effect of nanomaterials but also antagonize the role of nanoplates.^{12,13} Further exploring the interaction mechanism between CuS nanoplates and cell autophagy are conducive to enhance the photothermal efficiency of CuS nanoplates and lay a theoretical basis for the photothermal therapy of advanced prostate cancer.

MATERIALS AND METHODS

Synthesis and Detection of CuS Nanoplates

For the synthesis, morphology analysis, phase analysis, spectral analysis, and photothermal conversion test, see References.¹⁴

Cell Culture and Cytotoxicity Assay

Normal human prostate epithelial cells (RWPE-1, purchased from American Type Culture Collection (ATCC)) were cultured in keratinocyte serum-free medium supplemented with 0.05 mg/mL bovine pituitary extract, 5 ng/mL epidermal growth factor, and 1% of penicillin-streptomycin. Prostate cancer cells, PC-3, and DU145 (purchased from Institute of Biochemistry and Cell Biology, Shanghai Institutes for Biological Sciences (SIBS), Chinese Academy of Sciences) were cultured in RPMI (Roswell Park Memorial Institute)-1640 with 10% of fetal bovine serum and 1% of penicillin-streptomycin. The medium was changed every 2-3 days, and cells were passaged when growing to 80%-90% confluence. The cells that grew well were digested and adjusted to a density of 50,000 cells/mL. The cell suspension was then seeded in a 96-well plate, with 5000 cells (100 μ L of the suspension) in each well. The plate was beaten gently to blend the cells, and the old medium was removed after 24 hours of adherence. Medium containing different concentrations of CuS nanoplates was added,

treating for 24 hours, and then the medium was removed and the cells were washed 3 times with preheated Phosphate Buffer Saline (PBS). Then 100 μ L of medium and 10 μ L of CCK-8 solution was added in each well respectively, incubating at 37°C for 2 hours, and the absorbance of each well was detected using the microplate reader at the wavelength of 450 nm.

Photothermal Therapy of NIR-light-driven CuS Nanoplates Inducing the Necrosis of Prostate Cancer Cells

PC-3 and DU145 cells that grew well were passaged to a 24-well plate. Keeping adherence, the medium was removed when the confluence was about 50%. Medium containing different concentrations of CuS nanoplates was added, incubating for 24 hours. NIR irradiation was carried out, and the output power of the NIR instrument was adjusted to 0.51 W/cm², irradiating for 5 minutes at about 1 cm from the liquid surface. Then the medium was removed and the cells were washed 3 times with preheated PBS. Then 0.04% of trypan blue was added, staining for 5 minutes, the trypan blue solution was then removed, the cells were washed 3 times with PBS, and pictures were taken using a microscope.

PC-3 cells were digested and adjusted to the density of 50,000 cells/mL, and the cell suspension was seeded in a 96-well plate, with 5000 cells in each well. Four longitudinal lines from the 96-well plate were randomly selected and assigned to groups 1, 2, 3, and 4. The old medium was removed after 24 hours of adherence, and 40 μ M of chloroquine (CQ) was added to group 2 and group 4, pretreating for 12 hours. Then medium containing 120 μ g/mL of CuS was added to group 3 and group 4, treating for 24 hours, and the blank medium was added to group 1, as the control group. After 980 nm NIR irradiation was carried out, the output power of the NIR instrument was adjusted to 0.51 W/cm², irradiating for 5 minutes at about 1 cm from the liquid surface. The cells were washed 3 times with the preheated PBS then stained with live-dead staining and photographing. At the same time, 100 μ L of medium and 10 μ L of CCK-8 solution was added in each parallel well respectively, incubating at 37°C for 2 hours, and the absorbance of each well was detected using the microplate reader at 450 nm to reveal the amount of viable cells.

Detection of CuS Nanoplates Inducing Prostate Cancer Cell Autophagy

For the acridine orange staining, transmission electron microscopy, mCherry fluorescent labeling, and autophagy-related protein detection, see References.¹³

Photothermal Therapy of NIR-light-driven CuS Nanoplates in Nude Mouse With Prostate Cancer

All animal procedures were performed following the National Animal Experimentation guidelines and were approved by the ethics committee of the Shanghai Jiao Tong University. Four to 8-week-old nude male mice weighing 20-25 g were used. All mice were bred in aseptic conditions at a constant humidity and temperature with standard 12 hour light-dark cycles and free access to drinking water and standard chow. PC-3 cells were digested and resuspended in PBS, and the matrix was added at a volume ratio of 1:1 to make the cell density of 10 million cells/mL. The nude mice were anesthetized, and the prostates were localized in the root of seminal vesicles from the abdomen median incision. Then 20 μ L of cells (about 200,000) were injected with micro injectors, and the abdominal cavities were then closed. The tumor formation was observed and the nude mice were randomly divided into 4 groups, every group contains

5 mice. The tumor size was observed through ultrasonic testing at the third week, and PBS, 40 μM of CQ, 120 $\mu\text{g}/\text{mL}$ of CuS nanoplate suspension and CuS nanoplates plus CQ suspension were injected in the tumors of the 4 groups respectively, under ultrasound guidance. Twelve hours later, NIR light irradiation was given for 10 minutes, with an output power of 0.51 W/cm^2 . Meanwhile, the temperature was detected using a thermal imager. Treatment was given once a week, and after 3 weeks of photothermal therapy, the animals were sacrificed, samples were collected, pictures were taken, and hematoxylin-eosin (HE) staining was carried out to observe the therapeutic effects.

Statistical Analysis

SPSS 22.0 (SPSS Inc, USA) and Graph Pad Prism 5.0 software (Graph Pad Software, USA) were used to analyze the data and all values were expressed as mean \pm SD. Statistical analysis was performed by 1-way Analysis of Variance (ANOVA) followed by the Least—Significant Difference (LSD) or Dunnett's T3 posthoc test (where equal variances were not assumed) for multiple comparisons. All reported *P* values are 2-sided; **P* < .05, ***P* < .01.

RESULTS

Structure Identification and Properties Characterization of CuS

$\text{CuCl}_2 \cdot 2\text{H}_2\text{O}$ and $(\text{NH}_4)_2\text{S}$ were subjected to hydrothermal reaction at 160°C for 12 hours with polyvinyl pyrrolidone as the surfactant, and a dark green sample was obtained by centrifugal separation. It was identified to be hexagonal CuS nanoplates using scanning electron microscopy (Fig. 1A), transmission electron microscopy (Fig. 1B), and X-ray diffraction (Fig. 1C). The surface ligand of CuS was studied using FT-IR (Fig. 1D), and it was found that there was a broad peak of CuS surface ligand at 3437/cm, which was consistent with O—H stretching vibration of H_2O .

The NIR absorption spectra of CuS showed that the absorption at 1000 nm was the maximum (Fig. 1E); with fixed absorption spectra, the concentration of CuS nanoplates was positively correlated with the absorption of NIR light and the temperature, and finally a plateau occurred (Fig. 1F). The temperature increase of CuS nanoplates of 120 $\mu\text{g}/\text{mL}$ under the 980 nm laser irradiation with the power density of 0.51 W/cm^2 could reach up to 30° above, which was sufficient to meet the needs of tumor photothermal therapy.

NIR-light-driven CuS Nanoplates Could Inhibit the Growth of Prostate Cancer Cells in vivo and in vitro

The cytotoxicity detection of CuS nanoplates showed that there was no significant cytotoxicity when the concentration of CuS nanoplates was less than 160 $\mu\text{g}/\text{mL}$, and the survival rate of prostate epithelial cells after coculture for 24 hours and 48 hours was both more than 80%; when the concentration of CuS nanoplates reached 200 $\mu\text{g}/\text{mL}$, the survival rate of cells was less than 80%, indicating significant cytotoxicity (Fig. 2A and B, S2I). The in vitro results of CuS nanoplates photothermal therapy in treating prostate cancer showed that CuS nanoplates of 120 $\mu\text{g}/\text{mL}$ above could kill all the prostate cancer cells driven by 980 nm laser with a power of 0.51 W/cm^2 ; while CuS nanoplates of 80 $\mu\text{g}/\text{mL}$ could kill most of the tumor cells driven by 980 nm laser (Fig. 2C, S2J). Combined with the above cytotoxicity experimental data, the subsequent experiments were carried out in the presence of CuS at a concentration of 120 $\mu\text{g}/\text{mL}$.

CuS Nanoplates Inducing Autophagy of Prostate Cancer Cells

There was a granular change in PC-3 and DU145 cells when growing in the medium containing CuS nanoplates (Fig. 3A and B, S2A and B). Further transmission electron microscope test showed that the morphology of prostate cancer cells cultured in the medium without CuS nanoplates was regular, and there were more pseudopod and cytoplasmic organelles (Fig. 3C and D, S2C and D); while after treating with CuS nanoplates, the number of pseudopod and cytoplasmic organelles both reduced, and many circular phagocytic vesicle structures appeared in the cytoplasm, in which a large number of CuS nanoparticles and autophagosome-like structures were observed (Fig. 3E and F). The mCherry-LC3 syncytial virus labeling (Fig. 3H-3K, S2G and H), acridine orange staining (Fig. 3G, S2E and F), and autophagy protein test demonstrated that CuS induced the autophagy blockage of PC-3 cells (Fig. 3L), which was the same with CQ rather than rapamycin. So we chose CQ to block autophagy flux to discover whether inhibiting autophagy could enhance the efficacy of CuS nanoplates photothermal therapy in treating prostate cancer.

Inhibiting Autophagy Could Enhance the Efficacy of CuS Nanoplates Photothermal Therapy in Treating Prostate Cancer

Amazingly, for in vitro cultured prostate cancer cells, the addition of autophagic inhibitor could enhance the efficacy of CuS nanoplates photothermal therapy (Fig. S1A-D). The necrosis rate of cells in negative control group (the control group) was nearly 0%, and it was 46.50 \pm 0.06% and 66.77 \pm 0.04% in CuS group and CuS plus autophagic inhibitor group, respectively (Fig. S1E). There was a statistically significant difference between the control group and the latter 2 groups (*P* < .01).

To further evaluate the effect of CuS nanoplates photothermal therapy in treating prostate cancer, first, cultured PC-3 cells were used to induce in situ tumors in nude mice, when the tumor diameter increased to 0.5-1 cm, the nude mice were randomly divided into control (PBS) group, autophagic inhibitor (CQ) group, CuS group, and CuS plus autophagy inhibitor (CQ) group, CuS nanoplates and autophagy inhibitors were injected into the tumor under ultrasound guidance (Fig. 4A and B), and then under laser irradiation, the temperature change was detected with a thermal imager (Fig. 2D). After 3 weeks of laser irradiation, the experimental animals were sacrificed, and the tumor tissues were taken out for volume measurement and pathologic examination. The results showed that the tumor volume of PBS group, CQ group, CuS group, and CuS plus CQ group was 268 mm^3 , 240 mm^3 , 73 mm^3 , and 17 mm^3 , respectively. The statistical analysis indicated that the difference between PBS group and CQ group was not significant (*P* = .645), the difference between PBS group and CuS group was significant (*P* = .009), and the differences between CuS plus CQ group with PBS group, CQ group, and CuS group were all significant (*P* = .003, .006, and .038, respectively) (Fig. 4C and D). The pathologic examination showed no necrosis of tumor cells in PBS group and CQ group, while obvious cell necrosis in CuS group and CuS plus CQ group (Fig. 4E-H).

DISCUSSION

In response to the difficulties in treating mCRPC, photothermal therapy shows an encouraging prospect in the treatment of the primary lesion and bone metastatic

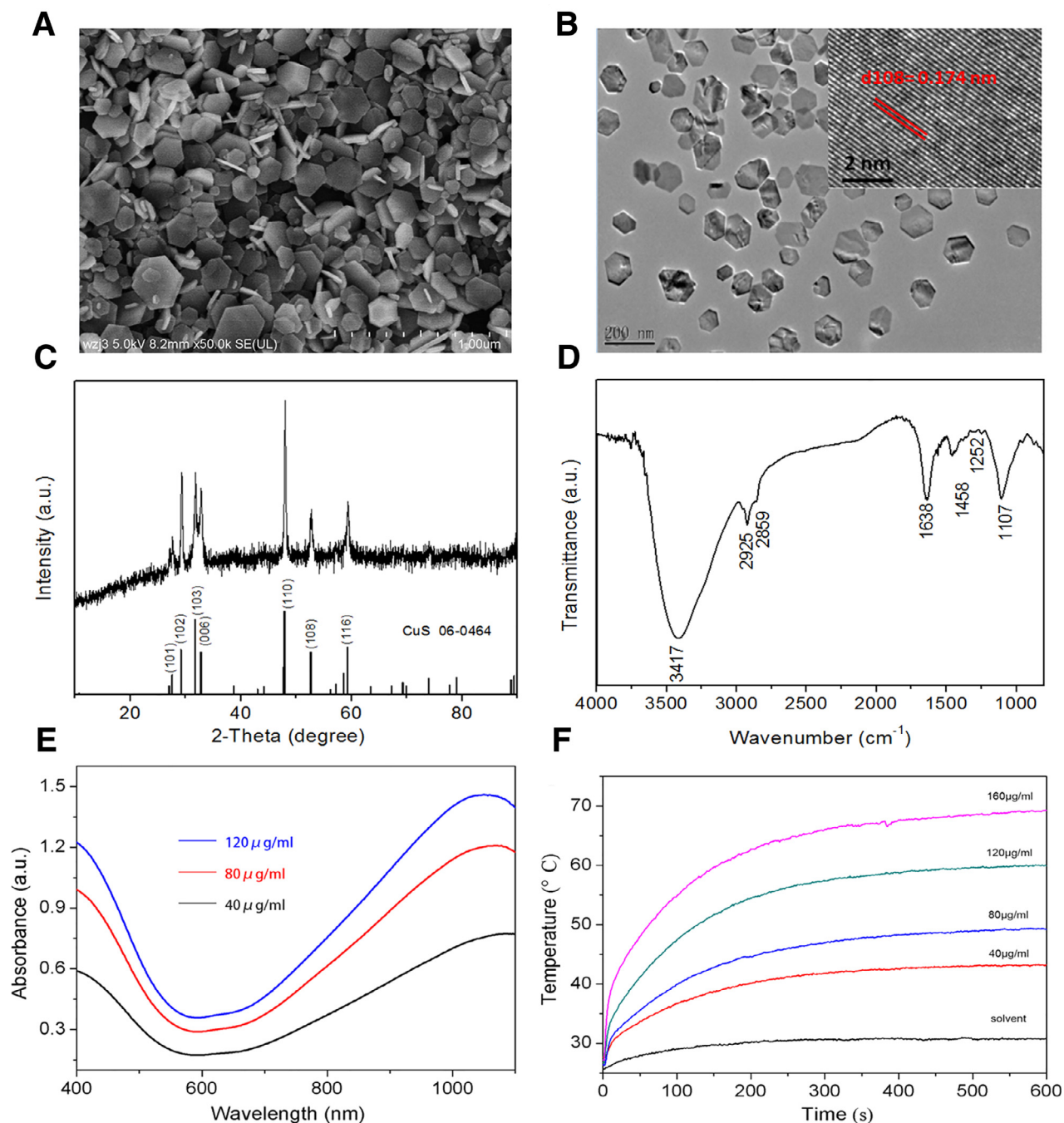


Figure 1. Structure identification and characterization of the copper sulfide (CuS) nanoplates. The scanning electron microscopy (A), transmission electron microscopy (B), and X-ray diffraction (C) showed that CuS was a flaky hexagon structure. The Fourier transform infrared spectroscopy showed that the surface of CuS nanostructures had PVP (polyvinyl pyrrolidone) ligands (D). The absorption of the nanoplates in the near infrared light was increased in the 600 nm-1000 nm area, and the highest absorption was near 1000 nm (E). The absorption rate and heating effect of recent infrared light were positively correlated with the concentration of CuS nanoplates (F). (Color version available online.)

lesions. Semiconductor nanoplates are preferred by simple preparation, low cost, and easy to be functionalized. The research of semiconductor photothermal conversion materials mainly focused on CuS-based compounds. Li et al¹⁵ reported the use of CuS in photothermal therapy for the first time, but the photothermal conversion efficiency of the CuS nanoparticles they produced was poor,

resulting in that the laser power density was far beyond the biosafety range, indicating a bleak application prospect.¹⁶

To optimize the photothermal properties of CuS nanoparticles, hexagonal CuS nanoplates were synthesized by hydrothermal method. The photothermal conversion efficiency of the nanoplates was significantly higher than

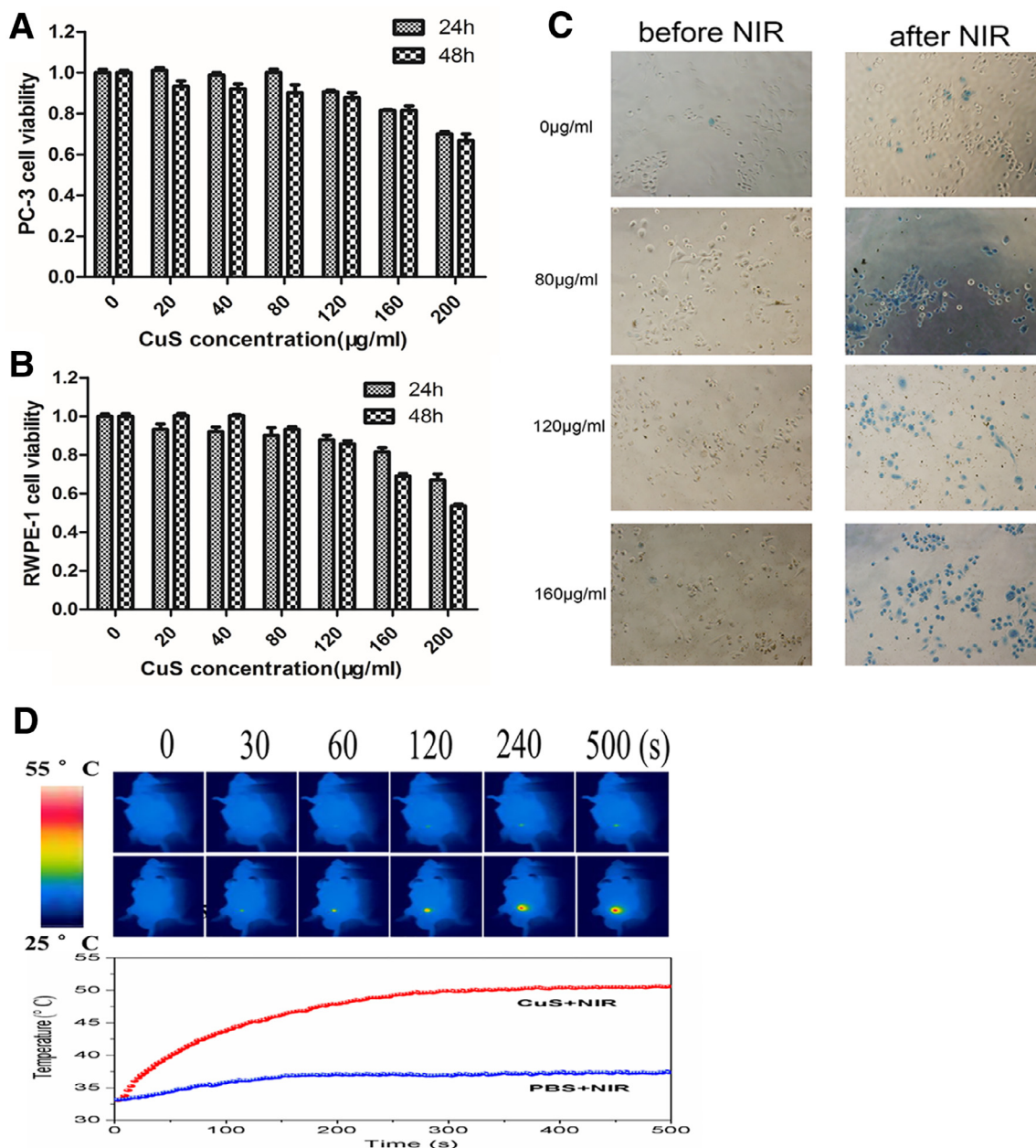


Figure 2. Effects of near-infrared light driving CuS nanoplates on the growth of prostate cancer cells. The effect of CuS nanoplates on the survival rate of prostate cancer PC-3 cells and RWPE-1 cells, when the concentration of CuS nanoplates was less than 160 µg/mL, the toxicity was low (**A and B**); 980 nm laser drives the photothermal inhibition of PC-3 cells, when the concentration of CuS nanoplates come to 120 µg/mL, almost all cancer cells were killed ($\times 200$) (**C**); thermal imager showed changes in tumor temperature in the experimental group of CuS and the control group of phosphate buffer (**D**). (Color version available online.)

that of nanoparticles. Both the *in vivo* and *in vitro* experiments indicated that NIR-light-driven CuS nanoplates could effectively inhibit the growth of prostate cancer cells. In addition, this hexagonal CuS nanoplates boast lower biotoxicity and a better application prospect.

Although in theory, photothermal therapy had a unique advantage in the treatment of solid tumors, the inefficient tissue-penetrating depth and excessive power density of laser constrained its further development.¹⁵ But with the advantages of deep tissue-penetrating and less

energy attenuation, NIR light could be the ideal light source of photothermal therapy in solid tumor treatment. The tissue-penetrating depth of 980 nm NIR light developed in this study was more than several centimeters.⁹ Previous studies had shown that the mCRPC bone metastatic lesions were located in areas close to body surface, including pelvis, spine bone, and ribs. The 980 nm NIR laser could have direct access to the primary lesion and metastatic lesions of prostate cancer through rectum or body surface, and thus it was the ideal light source of

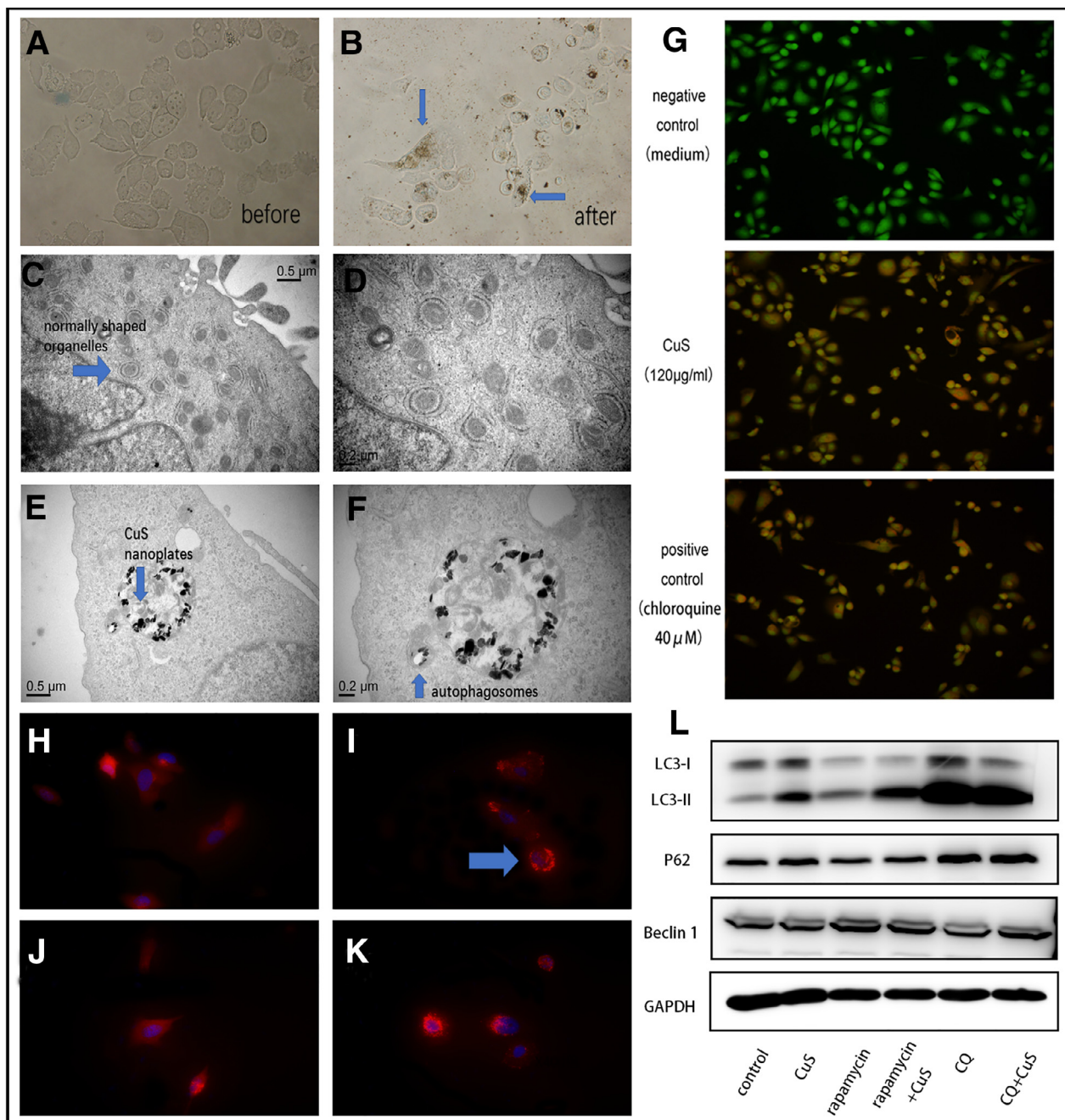


Figure 3. Detection of autophagy of prostate cancer cells induced by the CuS nanoplates. No granular change in PC-3 cells without CuS in medium ($\times 400$) (A) and granular changes in the PC-3 with CuS in medium ($\times 400$) (arrow) (B). Transmission electron microscopy showed the morphological rules of prostate cancer cells before the treatment of CuS nanoplates, and the normal organelles in the cytoplasm (C and D) were observed. When treated by CuS nanoplates, there appeared multiple round phagocytic vesicles in the PC-3 cells, which included the CuS nanoplates and multilayer membrane structures (autophagosome) (E and F). Acridine orange is a kind of double color fluorescent dyes, green fluorescence indicates the cellular structure, red fluorescence on behalf of the lysosome, the fusion of orange fluorescence represents autophagy-lysosome, in the picture, negative control group has only green fluorescence, and red fluorescence is very weak, while in positive control group (group chloroquine [CQ]), there is an obvious orange fluorescence, illustrates the autophagy-lysosome. For CuS intervention group, it appears the orange fluorescence similar with CQ group ($\times 200$) (G); PC-3 cells transfected with mCherry-LC3 virus, when there is no autophagy occurs, only visible red fluorescence evenly distributed in the cytoplasm, in the event of autophagy, red fluorescence gathered into pieces then formation of some massive red fluorescence spots, blue fluorescence 4',6-diamidino-2-phenylindole (DAPI) represent to nuclei. Red fluorescence evenly distributed in the cytoplasm with medium group ($\times 400$) (H) and autophagy inhibitor (3-MA) group ($\times 400$) (I), massive red fluorescence spots around the nucleus (arrow) can see in CuS group (J) and positive control group ($\times 400$) (rapamycin) (K); autophagy-related proteins LC3, P62, and beclin 1 change in CuS group compared with rapamycin and CQ (L). (Color version available online.)

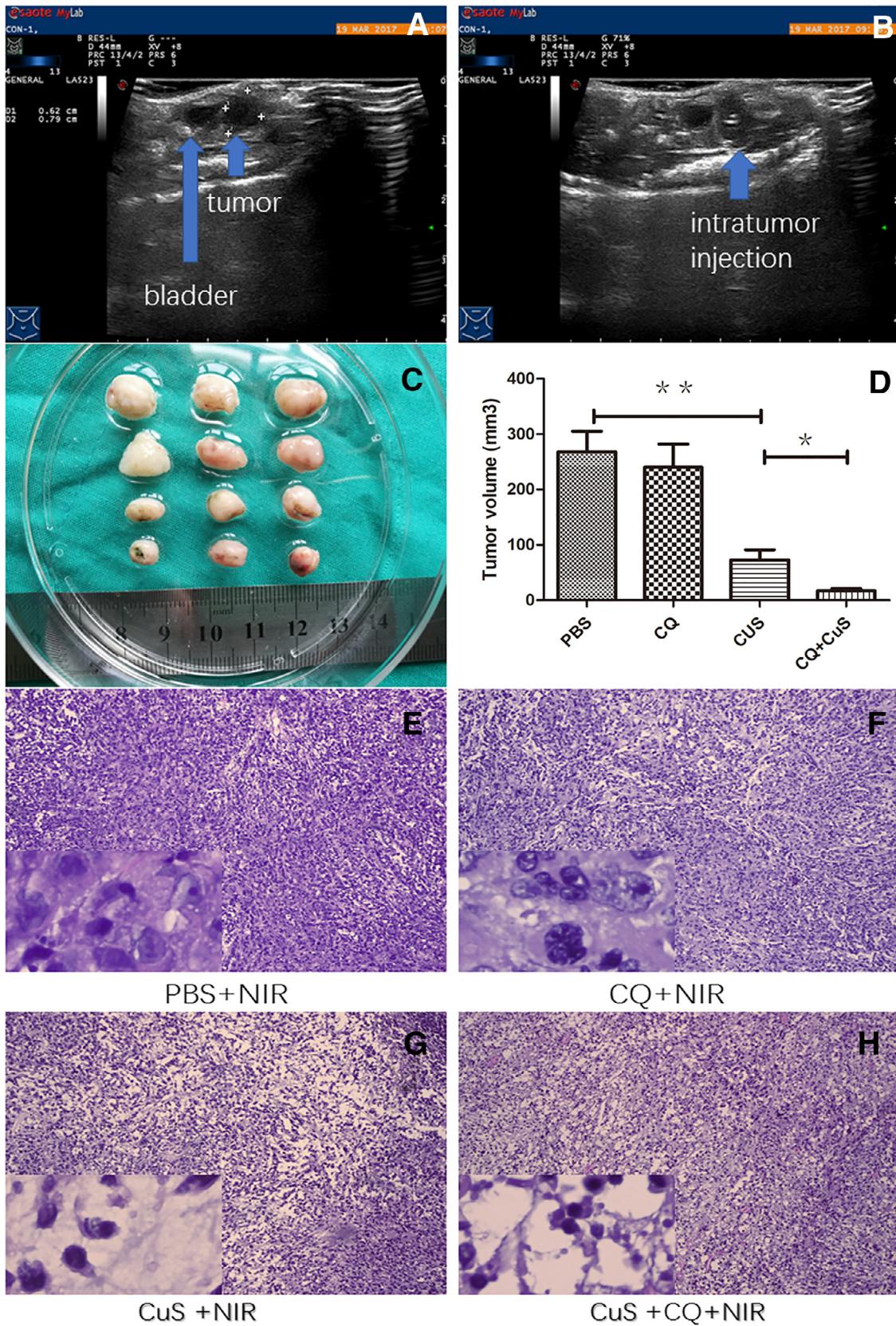


Figure 4. Inhibition of autophagy enhanced the photothermal therapy of the CuS nanoplates (in vivo). Type-B ultrasonic examination of prostate cancer (arrow) (A); intratumor injection of CuS nanoplates (arrow) (B) under the guidance of type-B ultrasound; the representative volume change of tumor (C and D) after 3 weeks of laser irradiation treated with nude mice, data between groups was statistically significant (* $P < .05$, ** $P < .01$), HE dyed results ($\times 100/\times 400$) (E, F, G, H) of the prostate in situ tumor to show the cell necrosis after laser irradiation. (Color version available online.)

mCRPC photothermal therapy. The experiment results showed that 980 nm NIR-light-driven CuS nanoplates could effectively inhibit the growth of prostate cancer cells in vivo and in vitro. But until now, almost all the experiments were conducted in the tumor injection or intravenous injection then get the thermal therapy, and the lack of a targeted approach that would provide for small number of cells to uptake the nanoplates and then be heated is a major limitation of the clinical application of the work presented.

In addition, in order to simulate the photothermal therapy of mCRPC using 980 nm NIR-light-driven CuS nanoplates, nude mice in situ tumor-inducing experiments were also carried out. CuS nanoplates were injected into the prostate tumor site under ultrasound guidance, and then NIR photothermal therapy was performed. The results showed that the program could effectively inhibit the prostate tumor growth and laid a preliminary foundation for subsequent clinical research.

Previous studies had found that a variety of nanoplates could cause cell autophagy, which can both enhance and antagonize the effect of nanomaterials. For example, silica nanoparticles cause autophagy and lead to impaired endothelium¹⁷; gold nanoparticles cause autophagy and cytoprotection of lung fibroblasts¹⁸; silver nanoparticles induce autophagy of cervical cancer cells, and inhibiting the autophagy enhance its anti-tumor effect¹³; thus, the mechanism of nanomaterials causing cell autophagy was yet to be further studied. It was found that CuS cause autophagy blockage of prostate tumor cells, and the intensity of autophagy blockage was positively correlated with the concentration of CuS. Inducing the autophagy blockage significantly enhance the inhibitory effect of CuS on prostate cancer cells. Therefore, it was speculated that CuS-induced autophagy blockage played a role in protecting prostate cancer cells, and the efficacy of CuS nanoplates photothermal therapy in treating advanced prostate cancer could be enhanced by regulating the autophagy, which was also demonstrated by the in vivo and in vitro experiments in this study.

CONCLUSION

CuS nanoplates are characterized by simple preparation, low biotoxicity, and high photothermal conversion efficiency. CuS nanoplates of 980 nm NIR-light-driven can significantly inhibit the progression of prostate cancer. Regulating autophagy can enhance the efficacy of CuS nanoplates photothermal therapy in the treatment of prostate cancer.

Acknowledgments. Jun Chen, Kai-le Zhang, and Xiao-yong Hu for cell culture, animal experiments, and article writing, Zhao-jie Wang and Zhi-gang Chen for material samples and

structure identification, Yan-jun Xu for type-B ultrasonic examination.

SUPPLEMENTARY MATERIALS

Supplementary material associated with this article can be found, in the online version, at <https://doi.org/10.1016/j.urology.2018.11.020>.

References

1. Siegel RL, Miller KD, Jemal A. Cancer statistics, 2016. *CA Cancer J Clin.* 2016;66:7–30.
2. Chen W, Zheng R, Baade PD, et al. Cancer statistics in China, 2015. *CA Cancer J Clin.* 2016;66:115–132.
3. Lipton A. Implications of bone metastases and the benefits of bone-targeted therapy. *Semin Oncol.* 2010;37(suppl 2):S15–S29.
4. Tannock IF, de Wit R, Berry WR, et al. Docetaxel plus prednisone or mitoxantrone plus prednisone for advanced prostate cancer. *N Engl J Med.* 2004;351:1502–1512.
5. Parker C, Nilsson S, Heinrich D, et al. Alpha emitter radium-223 and survival in metastatic prostate cancer. *N Engl J Med.* 2013;369:213–223.
6. Scher HI, Fizazi K, Saad F, et al. Increased survival with enzalutamide in prostate cancer after chemotherapy. *N Engl J Med.* 2012;367:1187–1197.
7. de Bono JS, Logothetis CJ, Molina A, et al. Abiraterone and increased survival in metastatic prostate cancer. *N Engl J Med.* 2011;364:1995–2005.
8. Dolmans DE, Fukumura D, Jain RK. Photodynamic therapy for cancer. *Nature Rev.* 2003;3:380–387.
9. Chen Z, Zhang L, Sun Y, Hu J, Wang D. 980-nm laser-driven photovoltaic cells based on rare-earth up-converting phosphors for biomedical applications. *Adv Funct Mater.* 2010;19:3815–3820.
10. Tian Q, Jiang F, Zou R, et al. Hydrophilic Cu9S5 nanocrystals: a photothermal agent with a 25.7% heat conversion efficiency for photothermal ablation of cancer cells in vivo. *ACS Nano.* 2011;5:9761–9771.
11. Chen Z, Wang Q, Wang H, et al. Ultrathin PEGylated W18O49 nanowires as a new 980 nm-laser-driven photothermal agent for efficient ablation of cancer cells in vivo. *Adv Mater.* 2013;25:2095.
12. Zhang Q, Yang W, Man N, et al. Autophagy-mediated chemosensitization in cancer cells by fullerene C60 nanocrystal. *Autophagy.* 2009;5:1107–1117.
13. Lin J, Huang Z, Wu H, et al. Inhibition of autophagy enhances the anticancer activity of silver nanoparticles. *Autophagy.* 2014;10:2006–2020.
14. Tian Q, Tang M, Sun Y, et al. Hydrophilic flower-like CuS superstructures as an efficient 980 nm laser-driven photothermal agent for ablation of cancer cells. *Adv Mater.* 2011;23:3542–3547.
15. Li Y, Lu W, Huang Q, Huang M, Li C, Chen W. Copper sulfide nanoparticles for photothermal ablation of tumor cells. *Nanomedicine.* 2010;5:1161.
16. Zhou M, Zhang R, Huang M, et al. A chelator-free multifunctional [64Cu]CuS nanoparticle platform for simultaneous micro-PET/CT imaging and photothermal ablation therapy. *J Am Chem Soc.* 2010;132:15351.
17. Duan J, Yu Y, Yu Y, et al. Silica nanoparticles induce autophagy and endothelial dysfunction via the PI3K/Akt/mTOR signaling pathway. *Int J Nanomed.* 2014;9:5131.
18. Li JJ, Hartono D, Ong CN, Bay BH, Yung LY. Autophagy and oxidative stress associated with gold nanoparticles. *Biomaterials.* 2010;31:5996–6003.